

Atom–Bond Pairwise Additive Representation for Halide–Benzene Potential Energy Surfaces: an Ab Initio Validation Study[#]

Margarita Albertí,^{*,†} Antonio Aguilar,[†] Josep M. Lucas,[†] Fernando Pirani,[‡] Cecilia Coletti,^{*,§} and Nazzareno Re[§]

IQTCUB, Departament de Química Física, Universitat de Barcelona, Barcelona, Spain, Dipartimento di Chimica, Università di Perugia, Perugia, Italy, and Dipartimento di Scienze del Farmaco, Università G. d'Annunzio, Chieti, Italy

Received: May 9, 2009; Revised Manuscript Received: June 9, 2009

The detailed knowledge of the basic aspects of molecular interactions and the representation of the involved potential energy surface in a proper analytical form are of paramount importance either to elucidate the nature of noncovalent interactions or to perform meaningful molecular dynamics simulations. To this aim, a recently developed semiempirical method, formulated in terms of atom/ion–molecular bond interactions, has been extended to investigate X^- – C_6H_6 systems ($X = F, Cl, Br, I$) and tested against highly correlated MP2 ab initio calculations. The role of the various components to the total interaction energy was also addressed by comparing the semiempirical contributions to their MP2 counterparts calculated using the symmetry adapted perturbation theory. The overall results, besides providing a more detailed picture of the interaction between anions and aromatic systems, pointed out that the current model is able to reproduce remarkably well the main features of the potential energy surface for the heavier X^- – C_6H_6 systems ($X = Cl, Br, I$), whereas for fluoride–benzene, the binding energies are underestimated as a consequence of the failure of the semiempirical method to describe the electrostatic interaction between a diffuse anion and a benzene at short range by means of a simple point charge model.

Introduction

Noncovalent intermolecular interactions¹ play an important role in chemistry and physics because they control the dynamics of several elementary processes occurring both in gaseous and condensed phases. These interactions typically arise from the balancing of several components, like the electrostatic (of either attractive or repulsive nature), the exchange (of repulsive nature) and the induction, dispersion, and charge transfer (of attractive nature). Unfortunately, it is rather difficult to accurately assess the relative role played by the various components of the interaction, some of them providing opposite contributions, and to determine the main features of the full potential energy surface. Therefore, it is often convenient to represent the global intermolecular interaction as a combination of a few terms to be considered representative of effective leading components. In particular, any molecular dynamics simulation requires the knowledge of the full intermolecular potential energy surface (PES) and the adoption of suitable functionals for its representation. A further challenging task is to provide a proper formulation of the dependence of the interaction components on the intermolecular distance and the geometry of the molecular aggregate because most of its configurations are often very weakly bound and, thus, quite difficult to characterize. For these reasons, it is worth spending significant theoretical and experimental efforts to determine in detail the intermolecular interaction features to build their modeling on sound molecular science foundations.

The investigation of the structure and dynamics of weakly bound clusters, with a particular attention to characterize the nature of the intermolecular interactions (see for instance refs 2, 3) and their role in molecular recognition and selection,^{1,3} is an expanding subject of research for its interest in several fields. In particular, how the behavior of prototype ion–aromatic molecule systems^{4,5} directly affects several chemical and physical processes occurring in biological systems.^{6–8}

During recent years, positive ions interacting with π electron cloud systems have been investigated in detail: alkaline or alkaline earth metal cation– π interactions having, in some cases, a strength comparable to that of chemical bonds,^{5,9–11} interactions between substituted benzenes, or simple heteroaromatic rings with complex cations.¹² π – π interactions have also been thoroughly studied.^{13,14} Much less attention has been devoted to anion–aromatic systems, although their interactions play an important role in organic synthesis,¹⁵ in solvation in heterogeneous media¹⁶ and in anion recognition processes,^{17,18} particularly in connection with the role of anion receptors in many biological systems.^{19,20} Only very recently, there has been a renewed interest in these kinds of interactions which can lead to a variety of binding patterns:²¹ the anion can bind to electron deficient aromatic rings in a “cation-like” fashion (i.e., along the C_{6v} symmetry axis)²² or can hydrogen bond to one or more hydrogens in an unsubstituted benzene (bz). The latter interaction is much less weak than what is generally assumed.²³ Halide–bz interactions, besides being of interest as prototypical systems for anion–aromatic binding, often occur in biological environments and, thus, play an important role in the modeling of such complex media. With the exception of high pressure mass spectrometry (HPMS) experiments^{24,25} on the whole family of halide–bz complexes, most of the experimental work has focused on chloride–bz clusters.^{26–28} On the theoretical side, a

[#] Part of the “Vincenzo Aquilanti Festschrift”.

* Corresponding authors. E-mail: m.alberti@ub.edu (M.A.); ccoletti@unich.it (C.C.).

[†] Universitat de Barcelona.

[‡] Università di Perugia.

[§] Università G. d'Annunzio.

TABLE 1: Halide Anion–Bond Interaction Parameters

ion-bond	$\epsilon_{\perp}/\text{kcal mol}^{-1}$	$\epsilon_{\parallel}/\text{kcal mol}^{-1}$	$r_{0\perp}/\text{\AA}$	$r_{0\parallel}/\text{\AA}$	β
F [−] –CC	0.484	1.636	3.399	3.671	6
F [−] –CH	0.822	0.890	3.186	3.379	6
Cl [−] –CC	0.378	1.375	3.832	4.073	7
Cl [−] –CH	0.588	0.660	3.655	3.839	7
Br [−] –CC	0.351	1.308	3.972	4.202	7
Br [−] –CH	0.532	0.602	3.808	3.990	7
I [−] –CC	0.317	1.221	4.166	4.380	7
I [−] –CH	0.466	0.535	4.018	4.198	7

recent high-level study reported binding energies and enthalpies calculated at the complete basis set (CBS) limit using MP2 and CCSD(T) levels of theory.²⁹

This paper focuses on the characterization and modeling of the interaction in X[−]–bz systems (X[−] = halide anion) by comparing results from semiempirical and accurate ab initio methods. The increasing research activity on molecular aggregates involving aromatic molecules has motivated the extension of an atom–bond-type formulation of the atom–molecule interaction, originally developed for rare gas (Rg)–bz systems,^{30,31} to ion–bz aggregates and has been recently applied to cation–bz systems.³² The most important features of this model are the simplicity of the potential formulation and the tight relationship existing between the potential parameters and some basic physical properties of the few body fragments of the overall molecular aggregate. Moreover, the atom–bond formulation of the interaction incorporates in a natural way three body effects. Extensive ab initio calculations at MP2/6-311++G** (3df,2pd) level of theory have been performed on these systems²⁹ and validated by MP2 complete basis set (CBS) calculations, and they are used here to test the interaction potential energy, at defined relative orientations of the X[−]–bz complexes, as a function of the intermolecular distance. Symmetry adapted perturbation theory (SAPT)³³ has also been employed to evaluate the contributions of the overall MP2 interaction energy in terms of electrostatic, exchange, induction, and dispersion components, enabling us to compare in detail the fundamental ingredients the semiempirical PES is based upon. Such a comparison is very useful to provide the accuracy of the proposed semiempirical method, to define its potentialities and limitations, and to improve its predictive power.

Semiempirical PES

As stressed above, a complete investigation of static and dynamical properties of molecular aggregates requires an

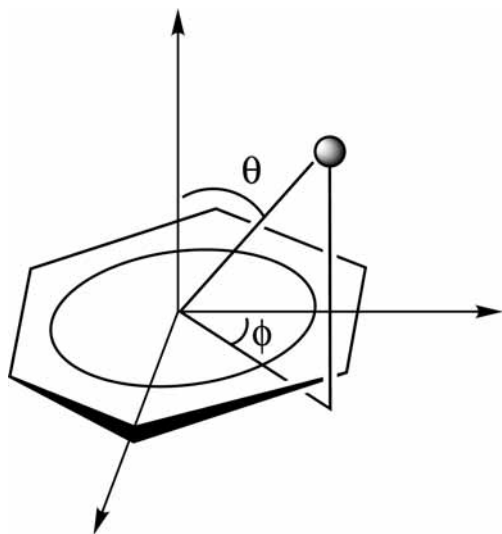


Figure 1. Polar coordinates R , θ , and ϕ defining the anion orientation with respect to the center of the bz ring.

accurate description of the whole PES. This makes it important to adopt a representation of the intermolecular potential energy, as a combination of a limited number of terms, represented by empirical or semiempirical functions having, as much as possible, a physical meaning. These terms should represent the leading components of the interaction, and at the same time, they should be considered as effective components because they include opposite contributions and effects due to the incomplete separability of the interaction energy. An important target of this study is, thus, to provide a functional representation of the PES that directly applies to the halogen anion series interacting with bz. However, the main advantage of the model is the interactions additivity that allows, as was indicated for alkali cation–bz systems,³² its generalization to systems of increasing complexity.

Following the basic ideas of our semiempirical method,^{30–32,34–37} the total intermolecular interaction potential, V , is assumed to depend on the combination of electrostatic and nonelectrostatic components. The nonelectrostatic component V_{nel} is constructed as a sum of 12 ion–bond contributions (6 X[−]–CC and 6 X[−]–CH), each one described by means of an improved version of the Lennard-Jones (ILJ) potential function,^{30,38} which removes most of inadequacies of the original version of the Lennard-Jones model (LJ). Each ion–bond term is then formulated as

$$V_{\text{ILJ}}(r, \alpha) = \epsilon(\alpha) \left[\frac{m}{n(r, \alpha) - m} \left(\frac{r_0(\alpha)}{r} \right)^{n(r, \alpha)} - \frac{n(r, \alpha)}{n(r, \alpha) - m} \left(\frac{r_0(\alpha)}{r} \right)^m \right] \quad (1)$$

where r represents the distance between the anion and the center of the bond, and α is the angle that the \mathbf{r} vector forms with the bond. The m parameter is taken equal to 4, the typical value for ion–neutral interactions. The well depth ϵ and the equilibrium distance r_0 are modulated through a simple trigonometric formula from the corresponding perpendicular and parallel components (see for instance ref 34) to obtain $\epsilon(\alpha)$ and $r_0(\alpha)$. The first term (positive) of eq 1 represents the size–repulsion contribution arising from each ion–bond pair, while the second one (negative) provides the induction plus dispersion effective attraction. The $n(r, \alpha)$ exponent, affecting the falloff of the ion–bond repulsion, is defined as

$$n(r, \alpha) = \beta + 4.0 \left(\frac{r}{r_0(\alpha)} \right)^2 \quad (2)$$

where β is an adjustable parameter related to the hardness of the interacting partners.^{30,38} Taking into account the higher polarizability of the X[−] ions with respect to that of corresponding isoelectronic positive alkali ions, the value of β has been assumed to be lower than 9–10, typical values of noncovalent interactions (more details on its choice are given in the Results and Discussion section). All the parameters of the X[−]–bond interactions (X[−]–CC and X[−]–CH) are reported in Table 1.

For all systems ϵ and r_0 values have been determined using the charge and the polarizability of the related atomic ion species as well as polarizability and effective polarizability tensor components of aromatic C–C and C–H bonds.^{30,34,39}

The electrostatic component of the interaction, V_{el} , has been evaluated, as in our previous studies of clusters containing ions and bz, considering the charge of the ion and an ensemble of

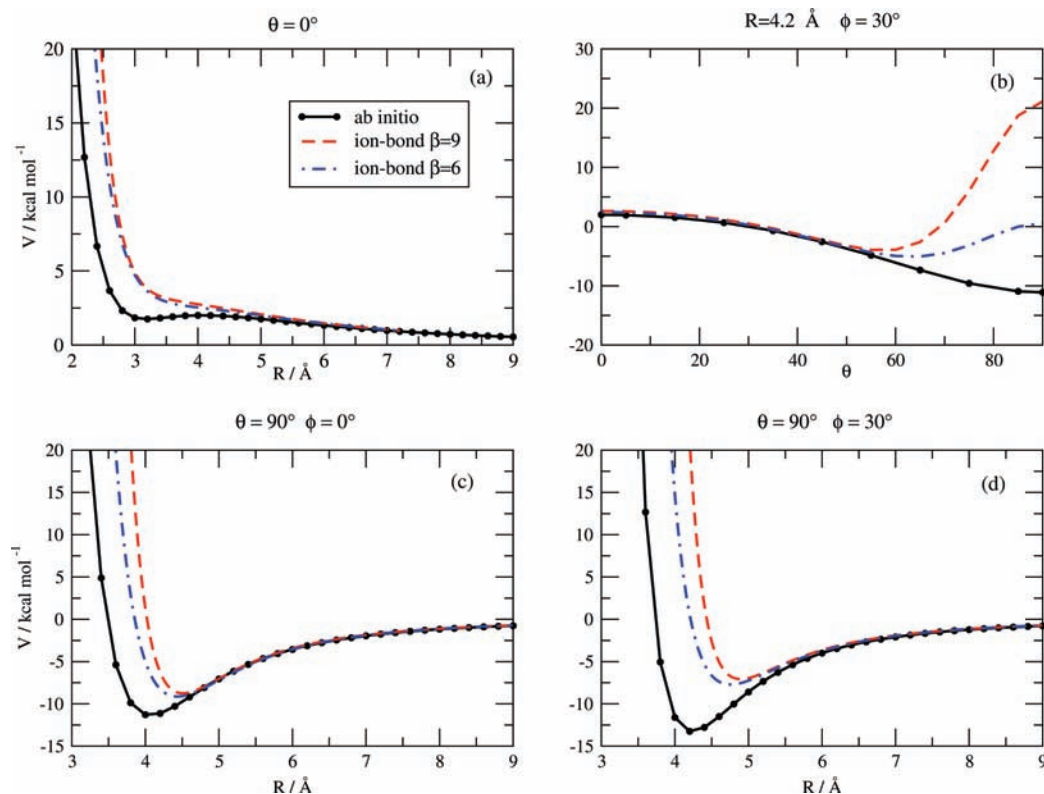


Figure 2. Potential energy curves at selected geometries for F^- -bz.

18 charge points distributed on the bz molecule frame (6 placed on the H atoms and the remaining 12 at fixed distances from C atoms on both sides of the aromatic ring). Such distribution has been chosen taking into account that V_{el} must asymptotically correspond to the ion-quadrupole interaction (see for instance ref 34). This leads to a charge of +0.09245 au on each H atom and to two negative charges of -0.04623 au separated by 1.905 Å on each C atom.

It is important to note that the present formulation of V involves the use of very few parameters, each one with a specific physical meaning. Furthermore, the usefulness of the adopted analytical form for V_{total} has been proved by recent molecular dynamics simulations.³⁴⁻³⁷ The obtained potential energy surface can be also expressed as a function of polar coordinates, R , representing the distance from the ion to the center of mass of the bz molecule, and the polar angles θ and ϕ , defining the X^- orientation with respect to bz (see Figure 1).³¹ The polar coordinates allow an easy identification of the most relevant configurations of the X^- -bz aggregates, such as the perpendicular one ($\theta = 0^\circ$), the linear one, where X^- approaches along the bz plane pointing toward an H atom ($\theta = 90^\circ$, $\phi = 30^\circ$), and the bifurcated one, with X^- pointing at the center of one of the CC bonds ($\theta = 90^\circ$, $\phi = 0^\circ$).

Ab Initio Calculations

The potential energy scans at the selected configurations were performed at MP2/6-311++G(3df,2pd) level of theory using Gaussian03.⁴⁰ This basis set was shown²⁹ to provide a good compromise between quality of results and computational load, as it contains a large number of multiple polarization functions to allow a good description of electron correlation, particularly important for binding in these kinds of systems. The basis sets employed in this work were all taken from Gaussian03 internal library with the exception of the 6-311++G(3df,2pd) basis set

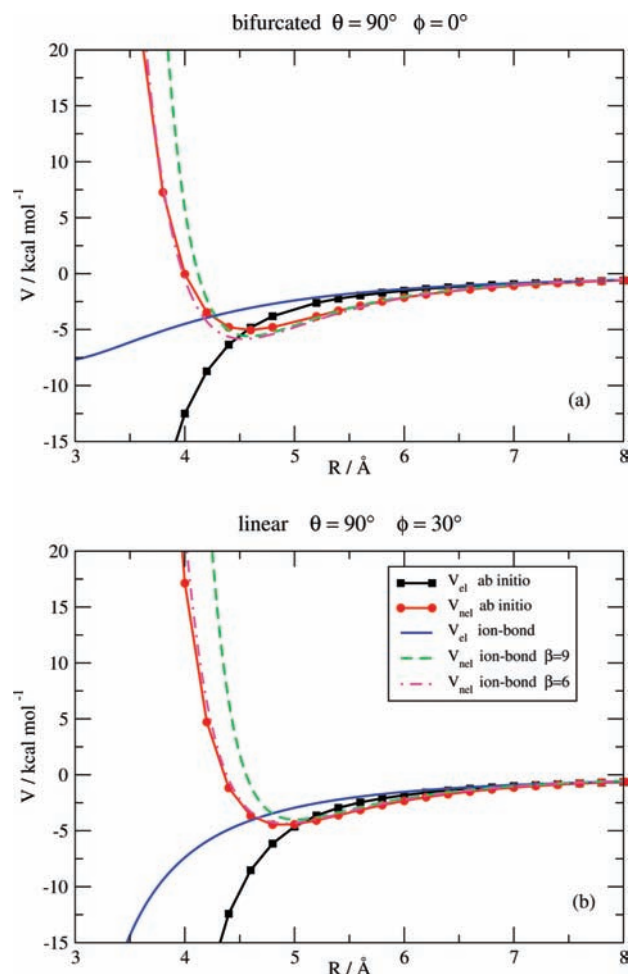


Figure 3. Electrostatic, V_{el} , and non electrostatic, V_{nel} , components of the potential energy for F^- -bz.

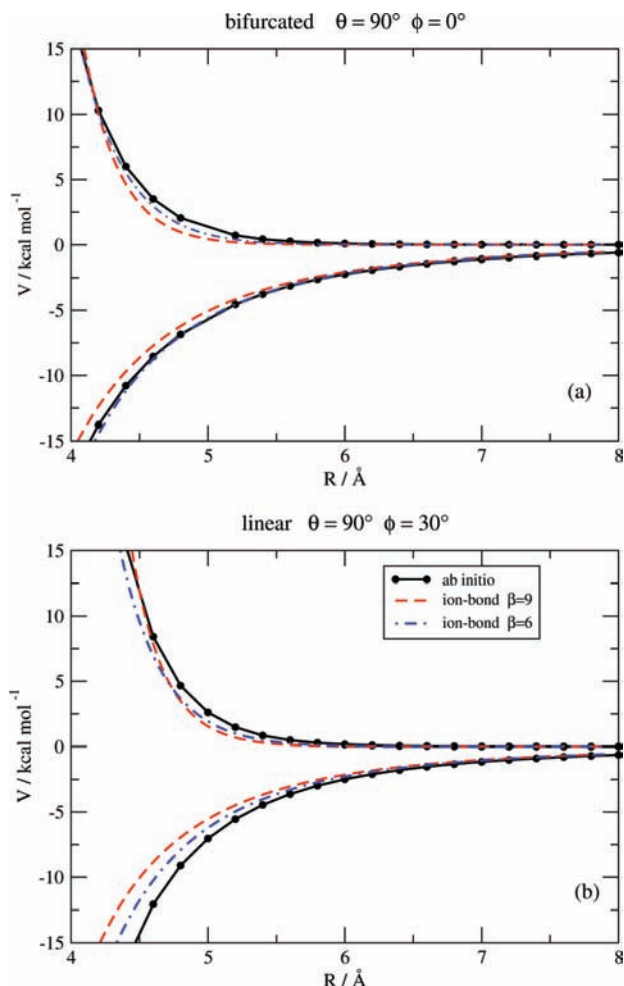


Figure 4. Attractive, $V_{\text{nel}}^{\text{att}}$, and repulsive, $V_{\text{nel}}^{\text{rep}}$, contributions to the nonelectrostatic (V_{nel}) component of the potential energy for F^- -bz.

for iodine, taken from ref 41. The basis set superposition error was evaluated at all points following Boys–Bernardi counterpoise (CP) correction method,⁴² and basis set superposition error (BSSE)-corrected geometry optimizations were carried out employing the CP corrected PES approach⁴³ implemented in Gaussian03. Potential energy scans at this level of theory were performed by initially optimizing the geometry of bz assuming a D_{6h} symmetry. The center of mass of the optimized structure was then taken as the center of a polar coordinate system placing the halide anion at a given radius R and polar angles θ and ϕ (see Figure 1).

To enable a detailed comparison between the semiempirical values for electrostatic and nonelectrostatic interaction contributions and the ab initio results, we have carried out an energy decomposition analysis for X^- -bz ($\text{X} = \text{F}, \text{Cl}, \text{Br}$) complexes according to the SAPT scheme,^{33,44} using the aug-cc-pVDZ basis set, to reduce the computational load. The interaction energy, using the second-order many-body perturbation theory SAPT2, can be represented as

$$E_{\text{int}} = E_{\text{el}}^{(1)} + E_{\text{exch}}^{(1)} + E_{\text{ind}}^{(2)} + E_{\text{disp}}^{(2)} + E_{\text{exch-ind}}^{(2)} + E_{\text{exch-disp}}^{(2)} + \delta_{\text{int}}^{\text{HF}} \quad (3)$$

where $E_{\text{el}}^{(1)}$ is the electrostatic interaction energy of the unperturbed monomers, $E_{\text{exch}}^{(1)}$ is the exchange repulsion energy due to the Pauli exclusion principle, $E_{\text{ind}}^{(2)}$ is the second-order attraction energy due

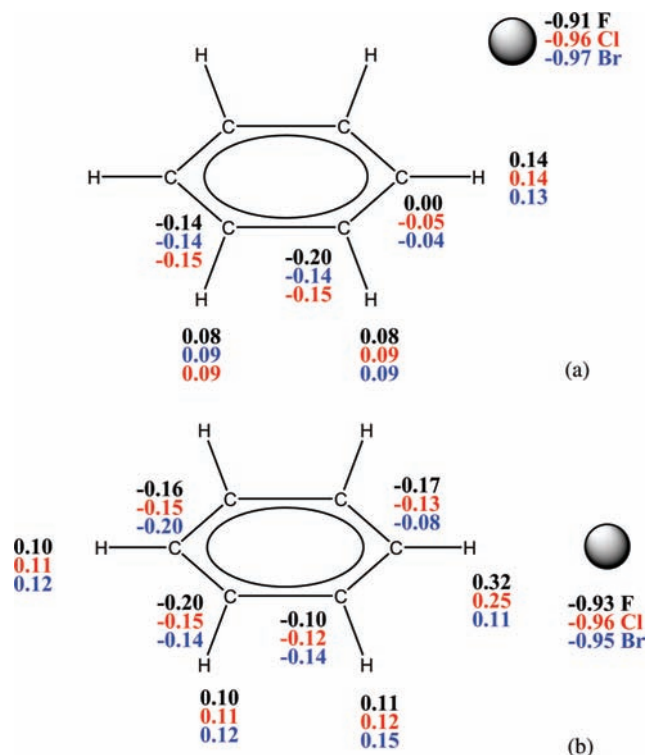


Figure 5. Atomic charges calculated according to the MP2 electronic density using Merz–Singh–Kollman scheme for the bifurcated (a) and linear (b) configurations.

to the induction interaction, $E_{\text{disp}}^{(2)}$ is the second-order dispersion energy, $E_{\text{exch-ind}}^{(2)}$ is the energy arising from the antisymmetrization of induction wave functions, $E_{\text{exch-disp}}^{(2)}$ represents the second-order correction for coupling between the exchange repulsion and the dispersion interaction, and $\delta_{\text{int}}^{\text{HF}}$ includes the higher-order induction and exchange corrections. BSSE corrections have been explicitly included in evaluating the SAPT interaction energies. We have combined some of these terms in order to define values that correspond to commonly understood physical quantities in the following way:

$$V_{\text{el}} = E_{\text{el}}^{(1)} \quad (4)$$

$$V_{\text{exch}} = E_{\text{exch}}^{(1)} \quad (5)$$

$$V_{\text{ind}} = E_{\text{ind}}^{(2)} + E_{\text{exch-ind}}^{(2)} + \delta_{\text{int}}^{\text{HF}} \quad (6)$$

$$V_{\text{disp}} = E_{\text{disp}}^{(2)} + E_{\text{exch-disp}}^{(2)} \quad (7)$$

Thus, the nonelectrostatic term corresponds to

$$V_{\text{nel}} = V_{\text{exch}} + V_{\text{ind}} + V_{\text{disp}} \quad (8)$$

This term can be further decomposed in its repulsion and attraction components, to allow a more detailed comparison with the semiempirical model:

$$V_{\text{nel}}^{\text{rep}} = V_{\text{exch}} \quad (9)$$

$$V_{\text{nel}}^{\text{attr}} = V_{\text{ind}} + V_{\text{disp}} \quad (10)$$

Results and Discussion

The comparison between the results derived from the semiempirical method and ab initio calculations has been carried out

for the whole family of X^- -bz complexes, and the intermolecular potential has been evaluated at four significant configurations in order to explore different zones of the PES: with X^- approaching bz along the C_{6v} bz symmetry axis and as a function of R ($\theta = 0^\circ$), fixing the values of ϕ and R ($R = R_{\text{eq}}$ and $\phi = 0^\circ$ or 30° , according to the most stable structure), and as a

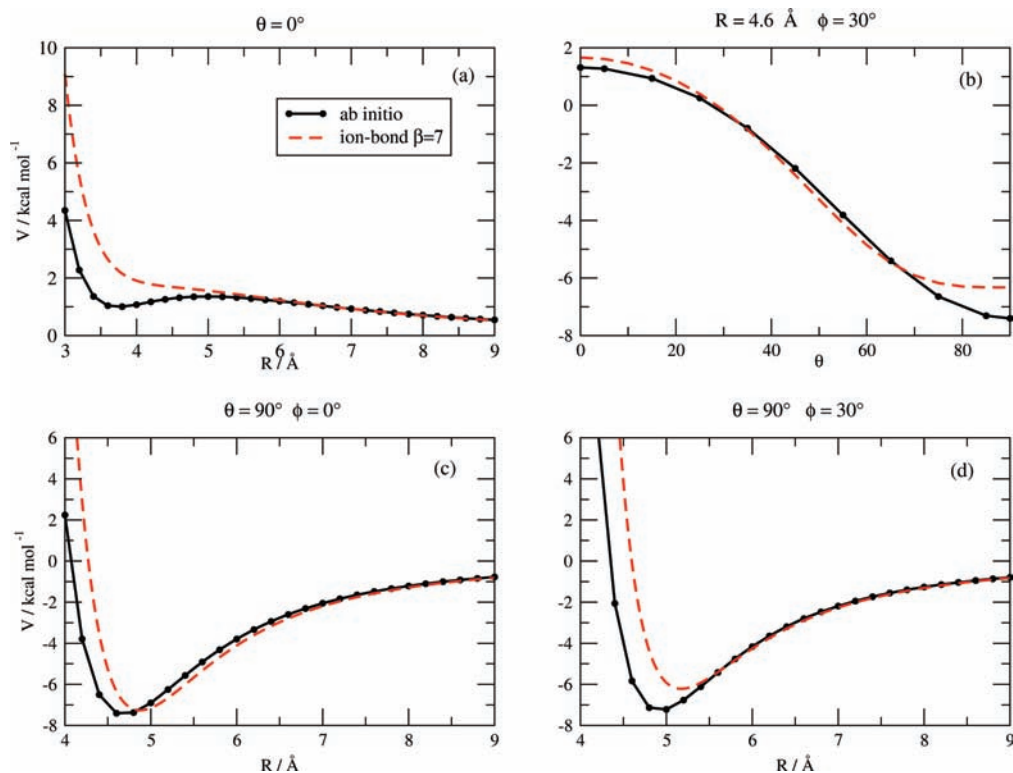


Figure 6. Potential energy curves at selected geometries for Cl^- -bz.

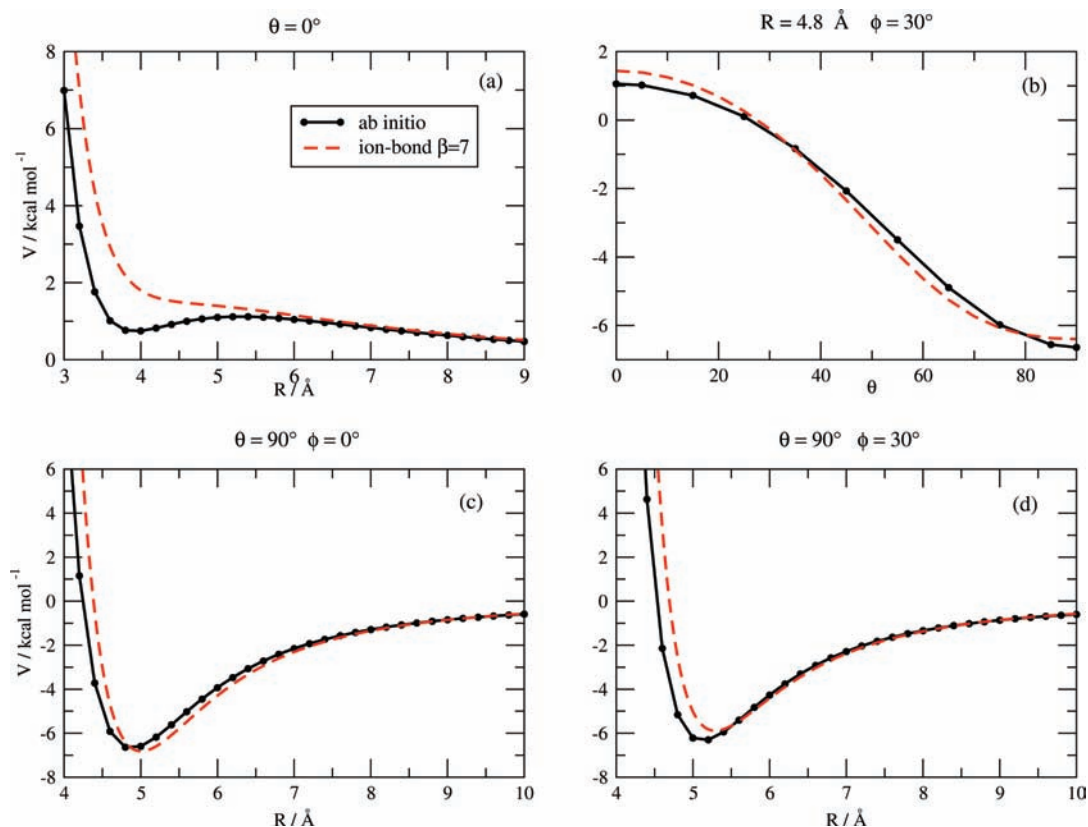


Figure 7. Potential energy curves at selected geometries for Br^- -bz.

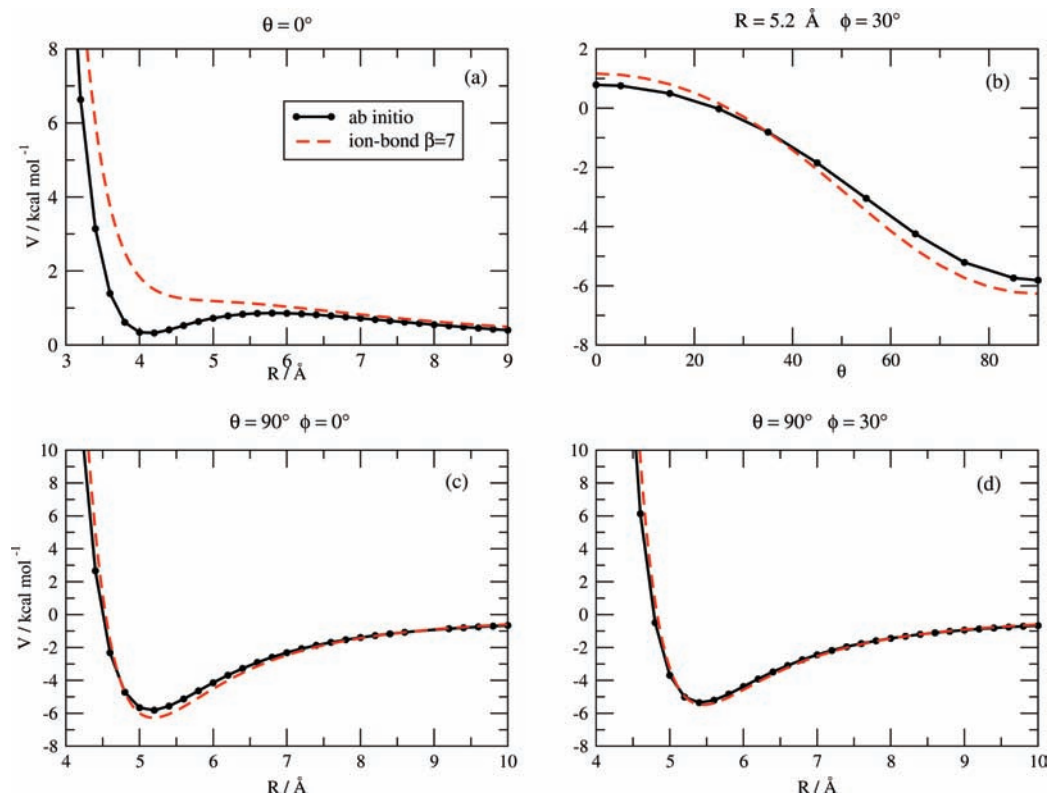


Figure 8. Potential energy curves at selected geometries for I^- -bz.

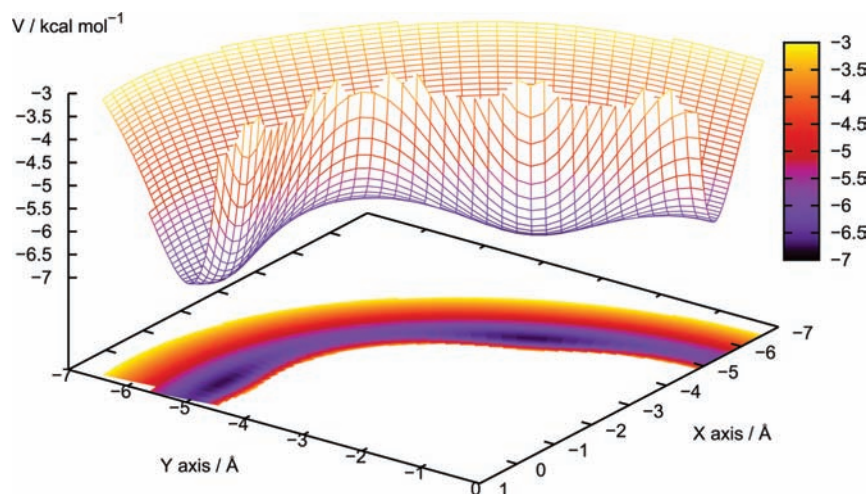


Figure 9. Semiempirical PES and contour plot for the in-plane geometry of Br^- -bz complex.

function of θ , when X^- approaches along the bz plane forming a bifurcated structure ($\theta = 90^\circ$ and $\phi = 0^\circ$) or a linear one ($\theta = 90^\circ$ and $\phi = 30^\circ$). The F^- -bz system will be discussed separately in order to define the limitations of the semiempirical representation and to devise possible strategies to overcome them. The remaining X^- -bz systems, presenting a more homogeneous behavior, will be treated jointly.

The F^- -bz system. Ab initio calculations and semiempirical predictions for the F^- -bz system, obtained by using two different values of the β parameter, are reported in Figure 2. The comparison shows that the semiempirical method underestimates the binding energy of the F^- -bz aggregate, although the qualitative features of the full PES are correctly described (e.g., the perpendicular configuration shown in (a) is fully repulsive). In particular, as shown in (c) and (d), the equilibrium distance R_{cq} of the two minima, corresponding to the bifurcated and linear geometries, is larger for the semiempirical model than

for the ab initio results, and the relative depth of the wells, although comparable, is inverted. The perpendicular configuration (a) shows a better agreement and so does the curve in (b) for sufficiently out-of-plane interaction geometries ($\theta < 60^\circ$). The comparison between the semiempirical results obtained with two different β values (see eq 2) shows an improvement for all configurations when using the smaller $\beta = 6$. This is somehow counterintuitive because β is related to the hardness of the ion, and one should expect larger β values in correspondence of the smaller halides. In order to shed light on this behavior and to investigate the limitations of the semiempirical model, we considered separately the electrostatic V_{el} and non electrostatic V_{nel} contributions for the in-plane configurations and compared them in Figure 3. The figure shows an excellent agreement for the nonelectrostatic part, in particular when using $\beta = 6$, whereas for the electrostatic component the ion-bond model fails to reproduce the ab initio results at $R < 5 \text{ \AA}$, although asymptoti-

TABLE 2: Bond Dissociation Energies (kcal mol⁻¹)

system	D_e model	D_e MP2/6-311++G(3df,2pd) ^a	D_e CCSD(T)/CBS ^a	D_0 CCSD(T)/CBS ^a	ΔH_{298}^0 CCSD(T)/CBS ^a	D_0 expt.	ΔH_{298}^0 expt.
F ⁻ -bz (bifurcated)	9.2	12.5	13.5	13.8	14.4		
F ⁻ -bz (linear)	7.7	14.1	15.0	15.2	15.3		15.3 ^b
Cl ⁻ -bz (bifurcated)	7.3	7.8	8.4	8.3	8.3	8.1 ^d	9.4 ^c
Cl ⁻ -bz (linear)	6.2	7.4	8.0	7.9	7.0		
Br ⁻ -bz (bifurcated)	6.8	6.9	7.4	7.3	7.3		9.0 ^c
Br ⁻ -bz (linear)	5.9	6.4	6.9	6.7	7.2		
I ⁻ -bz (bifurcated)	6.3	5.9	6.3	6.1	6.1		6.1 ^c
I ⁻ -bz (linear)	5.5	5.3	5.7	5.4	5.9		

^a ref 29. ^b ref 24. ^c ref 25. ^d ref 28.

cally the semiempirical and ab initio curve converge. This discrepancy is most probably due to the representation of the electrostatic potential through a fixed point charge model, which at short R cannot account for the behavior of the large anion electron cloud. Such conclusion is supported by the analysis of the ab initio electrostatic component for the other halide ions complexes (figures S1 and S2 in Supporting Information): In general, the attraction begins at larger values of R as the halide becomes heavier, i.e., when the electron cloud is larger. It is worth noting that, although the discrepancy in the electrostatic contribution between the semiempirical and ab initio results grows at small R values for heavier halides, its importance on the overall potential has consequences only for fluoride, and, to a much lesser extent, for chloride, which present minimum geometries at smaller R values. For the other halides, the discrepancy becomes significant when the repulsive part of V_{nel} is already dominant and, thus, has very little effect on the global interaction energy. Another element supporting this explanation for the different behavior of the electrostatic component comes from the comparison with the analysis of the same contribution in cation-bz interaction. In a recent work,³² the authors showed that for Na⁺-bz (isoelectronic with F⁻-bz) there is a very good agreement in the electrostatic contribution between the predictions of semiempirical model and ab initio results. The point charge electrostatic representation is indeed more bound to fail when large diffuse anions are involved in the interaction, whereas for small contracted cations, it is expected to lead to reasonably good results.

The excellent agreement of the nonelectrostatic component of the interaction energy, in particular for $\beta = 6$, and the reasons for the adoption of such an “anomalous” value for F⁻-bz have led us to perform a more stringent comparison with the ab initio results, by considering the two components of V_{nel} , i.e. the size-repulsion contribution and the effective plus induction attraction. The results are reported in Figure 4 and again show a very good agreement when $\beta = 6$, whereas the curves obtained with $\beta = 9$ show that the attractive part of V_{nel} is slightly underestimated, especially when R decreases. This feature can be ascribed to the presence of a charge transfer effect, which cannot be directly reproduced by the semiempirical model. Indeed, the calculation of atomic charges of the various complexes using the MP2 electron density following a Merz-Singh-Kollman scheme⁴⁵ showed that such an effect has some importance for the F⁻-bz complex, becoming negligible for the other halides (Figure 5). The contribution to $V_{\text{nel}}^{\text{att}}$ potential due to charge transfer can be indirectly taken into account in the ion-bond approach by lowering the value of β to 6 for F⁻-bz. However, for heavier halide complexes charge transfer plays a very little role and, thus, β is expected to assume a value typical of noncovalent interactions between partners with a high polarizability. We will, thus, use $\beta = 7$ for all the remaining halides. For chloride, this

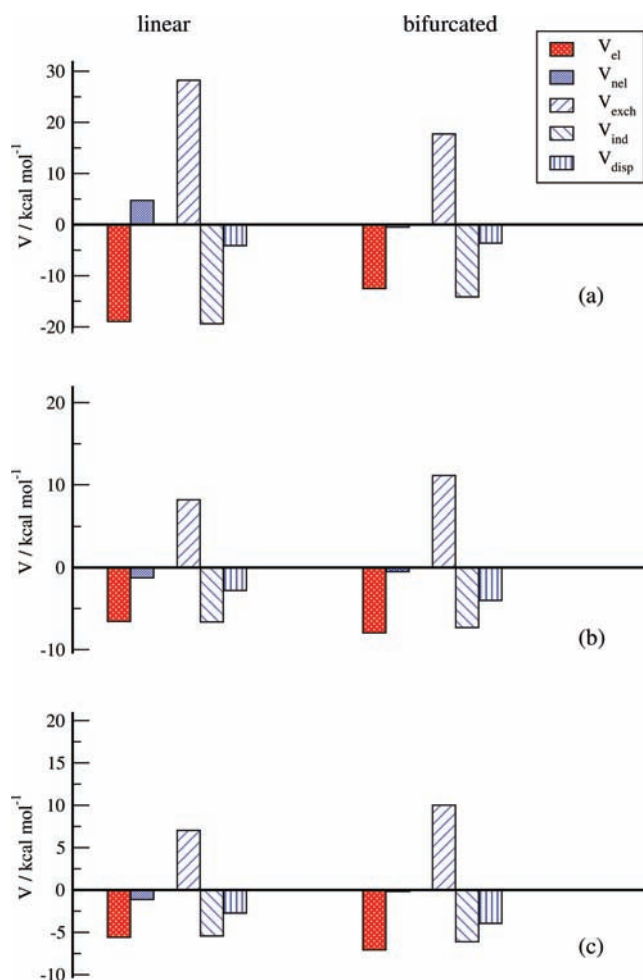


Figure 10. Electrostatic, V_{el} , and non electrostatic, V_{nel} , potential energy components for the linear and bifurcated minimum geometries for F⁻-bz (a), Cl⁻-bz (b) and Br⁻-bz (c). The V_{nel} component was further decomposed into its exchange, V_{exch} , induction, V_{ind} , and dispersion, V_{disp} , contributions. All the contributions to the total MP2 interaction energy were calculated according to the SAPT2 scheme.

value is a little smaller than expected to provide for the small charge transfer, whereas for bromide and iodide, this is the natural value for large polarized ions.

The X⁻-bz system (X = Cl, Br, I). We have reported in Figures 6–8 the potential energy data obtained for Cl⁻-bz, Br⁻-bz, and I⁻-bz, respectively. The agreement between the ion-bond and ab initio results improves as the halide becomes heavier, and it is especially remarkable for I⁻-bz system. As pointed out in the discussion for F⁻-bz, this is related to the diminished importance of the electrostatic contribution at low values of R to the overall potential as the halide grows larger (see also figures S1 and S2 in Supporting Information). Thus,

although for Cl^- -bz the interaction energy is still underestimated, in particular when considering the linear configuration, all the other geometries and/or systems show that the semiempirical potential is very close to the ab initio results, suggesting that it may be profitably used for molecular dynamics simulations.

A more quantitative examination can be made by comparing the prediction of the binding energies obtained with this model to those obtained with high level ab initio results and experimental data (Table 2). With the exception of the F^- -bz system, the binding energies for all the other systems are predicted reasonably well. Semiempirical results generally give less bound structures with smaller dissociation energies, D_e , and larger equilibrium distances (see also Figures 2 and 6–8), resulting from the short-range underestimation of V_{el} discussed above. The best agreement, at all geometries, is obtained for the heaviest Br^- -bz and I^- -bz systems, whose D_e values lie within 1 kcal mol $^{-1}$ and 0.5 kcal mol $^{-1}$, respectively, from the highly accurate CCSD(T) complete basis set (CBS) results.

Both qualitative and quantitative analysis, thus, lead to conclude that the present semiempirical model produces results in very good agreement with accurate ab initio predictions for the whole series of halide–bz complexes, with the exception of F^- -bz. This is quite striking when considering the simplicity of the semiempirical method and the fact that no ab initio calculations have been made to fit the effective parameters of the potential. This model allows to obtain the whole potential energy surface (including all the unstable configurations) with no computational efforts, and this is crucial to carry out extensive molecular dynamics simulations.

Figure 9 shows a section of the potential energy surface calculated with the present approach and the related contour plot for the in-plane configuration of Br^- -bz. The minima at the bifurcated geometries are connected by saddle points corresponding to the linear structures. The related barriers amount to only 0.9 kcal/mol. Ab initio frequency calculations at the high MP2/aug-cc-pVTZ level of theory for the X^- -bz systems ($\text{X} = \text{Cl}, \text{Br}, \text{I}$) indeed present a very small negative frequency value ($|\nu| < 30 \text{ cm}^{-1}$), which identifies these structures as saddle points in a very shallow region.

Origin of Binding in Halide-Bz Systems. We have further investigated in detail the interaction energy components at the minima of the potential energy curves for X^- -bz ($\text{X} = \text{F}, \text{Cl}$ and Br), through the SAPT2 method and the results are shown in Figure 10.

For all systems, the major contribution to the interaction energy comes from the electrostatic component, V_{el} , with a smaller nonelectrostatic contribution, V_{nel} . The latter is made of a large exchange repulsive contribution, V_{exch} , a still quite large induction, V_{ind} , and a smaller dispersion, V_{disp} , components. These two attraction terms nearly compensate the exchange repulsion. V_{exch} is particularly large for F^- -bz linear structure, while exhibiting a comparable contribution for Cl^- -bz and Br^- -bz complexes. V_{ind} and V_{disp} , with the exception of F^- -bz, again give similar contributions.

As a consequence, binding in the F^- -bz system mainly comes from the interplay between V_{exch} on one side and V_{el} and V_{ind} components on the other, producing a minimum at very short interaction distances. It is worth noting that for the linear F^- -bz complex the non electrostatic contribution to the total interaction energy is positive at the minimum interaction distance. It is, thus, not surprising that the present ion-bond model, which fails to reproduce V_{el} at short range, leads to much less bound and more loose complexes.

The other systems are more homogeneous with a V_{nel} , always giving a small negative contribution to the interaction potential, resulting in a more stable bifurcated configuration. In the ion-bond model (see figures S1 and S2 in Supporting Information), the electrostatic component is slightly underestimated, but this is compensated by a small overestimation of the non electrostatic component, producing a remarkable agreement of the total interaction energy.

Conclusions

The current study critically analyzes the performance of an ion-bond semiempirical model to predict the potential energy surface for halide–bz complexes. Such a model was shown to adequately reproduce the PES in rare gas–bz and alkali metal cation–bz systems. The comparison was made against accurate ab initio data, obtained with the highly correlated MP2 method, and large basis sets. In addition, all the physical contributions to the interaction energy in the semiempirical model were compared to their ab initio MP2 counterparts, calculated by the SAPT scheme. This has enabled us not only to test the validity of the adopted decomposition procedure and to highlight the possible failures but to understand the reasons and, in some cases, to propose remedies to correct these discrepancies.

The outcome of such an analysis led to very satisfactory results: (i) The nonelectrostatic component of the interaction energy is very close in both models; significant differences only arise when charge transfer effects play some role. However, their contribution, quite small in any case, is significant only for fluoride, and, to a much lesser extent, for chloride, and can be indirectly taken into account in the semiempirical model by changing the value of the parameter β . (ii) The ion-bond potential reproduces the electrostatic contribution correctly at large interaction distances but fails to do so at short range. This is due to the use of a point charge model which cannot describe the correct behavior of the large anion electron cloud. The difference in the electrostatic potential is, thus, more marked for heavier halides. In spite of this, such discrepancy is reflected in the value of the total interaction energy only when the electrostatic contribution, accounting for most of the binding energy, is overwhelming at short range, and this is the case only for the lightest halide. As a consequence, there is a good agreement between the semiempirical and ab initio potential energy surface both qualitatively and quantitatively, with the exception of the fluoride–bz system, for which however, the general topology of the PES is correctly reproduced. The agreement becomes excellent for bromide and iodide complexes.

The results confirm that for these systems it is possible to successfully use a simple and natural representation of the potential interaction energy to carry out meaningful molecular dynamics simulations.^{46,47} This is particularly important because, due to its additive nature, such a formulation can be readily extended to describe more complex systems.

Acknowledgment. M.A., A.A., and J.M.L. acknowledge financial support from the Ministerio de Educacion y Ciencia (Spain, project CTQ2007-61109) and the Generalitat de Catalunya-DURSI (project 2005 PEIR 0051/69). Thanks also are due to the Centre de Supercomputació de Catalunya CESCA-C4 and Fundació Catalana per a la Recerca for the allocated supercomputing time. F.P. acknowledges financial support from the Italian Ministry of University and Research (MIUR, PRIN 2005 contract no. 2004033958 and 2005033911-001). C.C. and N.R. acknowledge the Italian Ministry for University and Research for financial support (PRIN 2006 contract no. 2006038520).

Supporting Information Available: Figures S1 and S2, reporting semiempirical and ab initio V_{el} and V_{nel} components for the bifurcated and linear geometries as a function of R , for Cl^-bz and Br^-bz , respectively. This material is available free of charge via the Internet at <http://pubs.acs.org>.

References and Notes

- Müller-Dethelfs, K.; Hobza, P. *Chem. Rev.* **2000**, *100*, 143.
- Alonso, J. L.; Antolínez, S.; Bianco, S.; Lesarri, A.; López, J. C.; Caminati, W. *J. Am. Chem. Soc.* **2004**, *126*, 3244.
- Aquilanti, V.; Cornicchi, E.; Moix Teixidor, M.; Saendig, N.; Pirani, F.; Cappelletti, D. *Angew. Chem., Int. Ed.* **2005**, *44*, 2336.
- Dougherty, D. A. *Science* **1996**, *271*, 163.
- Ma, J. C.; Dougherty, D. A. *Chem. Rev.* **1997**, *97*, 1303.
- Cabarcos, O. M.; Weinheimer, C. J.; Lisy, J. M. *J. Chem. Phys.* **1998**, *108*, 5151.
- Cabarcos, O. M.; Weinheimer, C. J.; Lisy, J. M. *J. Chem. Phys.* **1999**, *110*, 8429.
- Jalbout, A. F.; Adamowicz, L. *J. Chem. Phys.* **2002**, *116*, 9672.
- Gokel, G. W.; Barbour, L. J.; De Wall, S. L.; Meadows, E. S. *Coord. Chem. Rev.* **2001**, *222*, 127.
- Feller, D.; Dixon, D. A.; Nicholas, J. B. *J. Phys. Chem. A* **2000**, *104*, 11414.
- Coletti, C.; Re, N. *J. Phys. Chem. A* **2006**, *110*, 6563.
- Reddy, A. S.; Sastry, G. N. *J. Phys. Chem. A* **2005**, *109*, 8893.
- (a) Sinnokrot, M. O.; Sherrill, C. D. *J. Phys. Chem. A* **2006**, *110*, 10656. (b) Park, Y. C.; Lee, J. S. *J. Phys. Chem. A* **2006**, *110*, 5091.
- Wheeler, S. E.; Houk, K. N. *J. Am. Chem. Soc.* **2008**, *130*, 10854.
- (a) Li, Y.; Flood, A. H. *J. Am. Chem. Soc.* **2008**, *130*, 12111. (b) Alcalde, E.; Mesquida, N.; Vilaseca, M.; Alvarez-Rúa, C.; García-Granda, S. *Supramol. Chem.* **2007**, *19*, 501.
- Cerichelli, G.; Mancini, G. *Langmuir* **2000**, *16*, 182.
- Mascal, M.; Armstrong, A.; Bartberger, M. D. *J. Am. Chem. Soc.* **2002**, *124*, 6274.
- Schneider, H.; Vogelhuber, K. M.; Shinle, F.; Weber, J. M. *J. Am. Chem. Soc.* **2007**, *129*, 13022.
- Bianchi, A.; Bowman-James, K.; García-España, E. (Eds.) *Supramolecular Chemistry of Anions*, Wiley, 1997.
- Imai, Y. N.; Inoue, Y.; Nakanishi, I.; Kitaura, K. *Protein Sci.* **2008**, *17*, 1129.
- Hay, B. P.; Bryantsev, V. S. *Chem. Commun.* **2008**, *21*, 2393.
- (a) Hiraoka, K.; Mizuse, S.; Yamabe, S. *J. Phys. Chem.* **1987**, *91*, 5294. (b) Quiñonero, D.; Frontera, A.; Garau, C.; Ballester, P.; Costa, A.; Deyà, P. M. *ChemPhysChem* **2006**, *7*, 2487. (c) Frontera, A.; Quiñonero, D.; Costa, A.; Ballester, P.; Deyà, P. M. *New. J. Chem.* **2007**, *31*, 556.
- Bryantsev, V. S.; Hay, B. P. *J. Am. Chem. Soc.* **2005**, *127*, 8282.
- Hiraoka, K.; Mizuse, S.; Yamabe, S. *J. Chem. Phys.* **1987**, *86*, 4102.
- Hiraoka, K.; Mizuse, S.; Yamabe, S. *Chem. Phys. Lett.* **1988**, *147*, 174.
- Loh, Z. M.; Wilson, R. L.; Wild, D. A.; Bieske, E. J.; Zehnacker, A. *J. Chem. Phys.* **2003**, *119*, 9559.
- Thompson, C. D.; Poad, B. L. J.; Emmeluth, C.; Bieske, E. J. *Chem. Phys. Lett.* **2006**, *428*, 18.
- Tschurl, M.; Ueberfluss, C.; Boesl, U. *Chem. Phys. Lett.* **2007**, *439*, 23.
- Coletti, C.; Re, N. *J. Phys. Chem. A* **2009**, *113*, 1578.
- Pirani, F.; Albertí, M.; Castro, A.; Moix, M.; Cappelletti, D. *Chem. Phys. Lett.* **2004**, *394*, 37.
- Albertí, M.; Castro, A.; Laganà, A.; Pirani, F.; Porrini, M.; Cappelletti, D. *Chem. Phys. Lett.* **2004**, *392*, 514.
- Albertí, M.; Aguilar, A.; Lucas, J. M.; Pirani, F.; Cappelletti, D.; Coletti, C.; Re, N. *J. Phys. Chem. A* **2006**, *109*, 9002.
- Jeziorski, B.; Moszynski, R.; Szalewicz, K. *Chem. Rev.* **1994**, *94*, 1887.
- Albertí, M.; Castro, A.; Laganà, A.; Moix, M.; Pirani, F.; Cappelletti, D.; Liuti, G. *J. Phys. Chem. A* **2005**, *110*, 9002.
- Albertí, M.; Aguilar, A.; Lucas, J. M.; Laganà, A.; Pirani, F. *J. Phys. Chem. A* **2007**, *111*, 1780.
- Huarte-Larragaña, F.; Aguilar, A.; Lucas, J. M.; Albertí, M. *J. Phys. Chem. A* **2007**, *111*, 8072.
- Albertí, M.; Aguilar, A.; Lucas, J. M.; Cappelletti, D.; Laganà, A.; Pirani, F. *Chem. Phys.* **2006**, *328*, 221.
- Pirani, P.; Brizi, S.; Roncaratti, L. F.; Casavecchia, P.; Cappelletti, D.; Vecchiocattivi, F. *Phys. Chem. Chem. Phys.* **2008**, *10*, 5489.
- Pirani, F.; Cappelletti, D.; Liuti, G. *Chem. Phys. Lett.* **2001**, *350*, 286.
- Frisch, M. J.; Trucks, G. W.; Schlegel, H. B.; Scuseria, G. E.; Robb, M. A.; Cheeseman, J. R.; Montgomery, Jr., J. A.; Vreven, T.; Kudin, K. N.; Burant, J. C.; Millam, J. M.; Iyengar, S. S.; Tomasi, J.; Barone, V.; Mennucci, B.; Cossi, M.; Scalmani, G.; Rega, N.; Petersson, G. A.; Nakatsuji, H.; Hada, M.; Ehara, M.; Toyota, K.; Fukuda, R.; Hasegawa, J.; Ishida, M.; Nakajima, T.; Honda, Y.; Kitao, O.; Nakai, H.; Klene, M.; Li, X.; Knox, J. E.; Hratchian, H. P.; Cross, J. B.; Bakken, V.; Adamo, C.; Jaramillo, J.; Gomperts, R.; Stratmann, R. E.; Yazyev, O.; Austin, A. J.; Cammi, R.; Pomelli, C.; Ochterski, J. W.; Ayala, P. Y.; Morokuma, K.; Voth, G. A.; Salvador, P.; Dannenberg, J. J.; Zakrzewski, V. G.; Dapprich, S.; Daniels, A. D.; Strain, M. C.; Farkas, O.; Malick, D. K.; Rabuck, A. D.; Raghavachari, K.; Foresman, J. B.; Ortiz, J. V.; Cui, Q.; Baboul, A. G.; Clifford, S.; Cioslowski, J.; Stefanov, B. B.; Liu, G.; Liashenko, A.; Piskorz, P.; Komaromi, I.; Martin, R. L.; Fox, D. J.; Keith, T.; Al-Laham, M. A.; Peng, C. Y.; Nanayakkara, A.; Challacombe, M.; Gill, P. M. W.; Johnson, B.; Chen, W.; Wong, M. W.; Gonzalez, C.; and Pople, J. A.; *Gaussian03 Revision C.02*; Gaussian, Inc.: Wallingford, CT, 2004.
- Begović, N.; Marković, Z.; Anić, S.; Kolar-Anić, L. *J. Phys. Chem. A* **2004**, *108*, 651.
- Boys, S. F.; Bernardi, R. *Mol. Phys.* **1970**, *19*, 553.
- Simón, S.; Duran, M.; Dannenberg, J. J. *J. Chem. Phys.* **1996**, *105*, 1104.
- Bukowski R.; Cencek, W.; Jankowski, P.; Jeziorska, M.; Jeziorski, B.; Lotrich, V. F.; Kucharski, S. A.; Misquitta, A. J.; Moszyński, R.; Patkowski, K.; Podeszwa, R.; Rybak, S.; Szalewicz, K.; Williams, H. L.; Wheatley, R. J.; Wormer, P. E. S.; Zuchowski, P. S. *SAPT 2006 Program Package*; University of Delaware and University of Warsaw: Newark, Delaware and ul. Pasteura 1, 02-093 Warsaw.
- Singh, U. C.; Kollman, P. A. *J. Comput. Chem.* **1984**, *5*, 129.
- Albertí, M.; Castro, A.; Laganà, A.; Moix, M.; Pirani, F.; Cappelletti, D. *Eur. Phys. J. D* **2006**, *38*, 185.
- Albertí, M.; Aguilar, A.; Lucas, J. M.; Pirani, F. *Theor. Chem. Acc.* **2009**, *123*, 21.